TRACKING OF CRACK SURFACES FOR THREE-DIMENSIONAL SDA MODELS

C. Feist and G. Hofstetter
Institute for Structural Analysis and Strength of Materials, University of Innsbruck, 6020 Innsbruck, Austria

ABSTRACT

A numerical model formulated within the framework of a nonsymmetric strong discontinuity approach (SDA) for fracture simulations of plain concrete represents the point of departure for the present study. The model based on the assumption of fixed cracks exploits the concept of the elements with embedded discontinuities. Discontinuity segments of individual elements are considered to form a C^0-continuous discontinuity surface. Enforcement of continuity across adjacent elements is established by a *partial domain tracking algorithm* (PDTA). Within the present work emphasis is put on the tracking of crack surfaces across three-dimensional discretizations for the SDA-model. A three-dimensional implementation of the PDTA is outlined and investigated by means of academic problems. Application of the algorithm to the tracking of an arbitrarily shaped 3D crack surface is demonstrated.

1 INTRODUCTION

The strong discontinuity approach (SDA) has gained wide popularity in numerical simulations of concrete fracture over the last years. The SDA starts from the formulation of the strong discontinuity kinematics which idealize the existence of a macroscopic crack as a discontinuity within the displacement field. It furthermore makes use of a special type of elements, termed as the elements with embedded discontinuities. These elements are characterized by the embedment of discontinuity segments within their element domains. The discontinuity segments can cross individual elements and consequently any spatial discretization of some solid in a nearly arbitrary way. Hence, in contrast to the classical smeared crack approach these elements allow a proper resolution of the kinematics related to macroscopic cracking and in contrast to discrete crack-models avoid the use of extensive remeshing.

In principle, the discontinuity segments found in individual elements could be placed within the respective element domains based solely on local information. This implies that in general these segments do not form a C^0-continuous discontinuity surface across adjacent elements. However, it is shown in [1], [2] that continuity of the discontinuity surface is mandatory in order to obtain objective results, i.e. results that do not depend on the employed discretization.

In order to enforce continuity of discontinuity surfaces, so called *tracking algorithms* [3] are used. A *local tracking algorithm* is based on geometric considerations whereas within the *global tracking algorithm* [3] the discontinuity surface is represented by the isosurface of a scalar field. Beside these two algorithms in [4] a *partial domain tracking algorithm* (PDTA) was proposed and the necessary steps were given for tracking of discontinuities across two-dimensional discretizations. The present work is primarily dedicated to its extension to three-dimensional problems. At first, however, the numerical model based on the SDA is outlined.

2 THE STRONG DISCONTINUITY APPROACH

2.1 The strong discontinuity kinematics

Consider a body $\mathcal{B}$ occupying a closed domain $\Omega \subset \mathbb{R}^3$, with material points whose locations are defined by $\boldsymbol{x} \in \Omega$. Let Ω be split by an internal discontinuity surface $\Gamma \subset \mathbb{R}^2$ – uniquely defined by its normal vector $\boldsymbol{n}$ – into two disjoint parts Ω^+ and Ω^-. In addition assume the existence of a

yet arbitrary subdomain $\Omega_\varphi \subset \Omega$ which serves as the support of a function $\varphi(\boldsymbol{x})$. The displacement field characterized by the presence of the discontinuity surface Γ is then decomposed as

$$\boldsymbol{u}(\boldsymbol{x}) = \bar{\boldsymbol{u}}(\boldsymbol{x}) + [H_\Gamma(\boldsymbol{x}) - \varphi(\boldsymbol{x})]\ [\![\boldsymbol{u}]\!](\boldsymbol{x}) \tag{1}$$

where H_Γ denotes the HEAVISIDE-function centered on Γ. Both, $\bar{\boldsymbol{u}}(\boldsymbol{x})$ and $[\![\boldsymbol{u}]\!](\boldsymbol{x})$ are smooth, continuous functions on Ω. The magnitude of the displacement jump across Γ – termed as $[\![\boldsymbol{u}]\!]_\Gamma$ – is given by the value of $[\![\boldsymbol{u}]\!]$ at the discontinuity such that $[\![\boldsymbol{u}]\!]_\Gamma = [\![\boldsymbol{u}]\!](\boldsymbol{x}) \quad \forall \boldsymbol{x} \in \Gamma$. Function $\varphi(\boldsymbol{x})$ in eqn (1) is used to restrict the effect of the displacement jump $[\![\boldsymbol{u}]\!]_\Gamma$ to domain Ω_φ which is established by postulating for $\varphi(\boldsymbol{x})$

$$\varphi(\boldsymbol{x}) = \begin{cases} 0 & \forall \boldsymbol{x} \in \Omega^- \setminus \Omega_\varphi^- \\ 1 & \forall \boldsymbol{x} \in \Omega^+ \setminus \Omega_\varphi^+ \\ C^0 - \text{continuous in interval } [0,\ 1] & \forall \boldsymbol{x} \in \Omega_\varphi \end{cases} . \tag{2}$$

Adopting the linearized kinematic relations the strain field follows from eqn (1) as

$$\boldsymbol{\varepsilon}(\boldsymbol{x}) = \boldsymbol{\nabla}^s \boldsymbol{u}(\boldsymbol{x}) = \underbrace{\boldsymbol{\nabla}^s \bar{\boldsymbol{u}}(\boldsymbol{x}) - ([\![\boldsymbol{u}]\!](\boldsymbol{x}) \otimes \boldsymbol{\nabla}\varphi(\boldsymbol{x}))^s}_{\bar{\boldsymbol{\varepsilon}}(\boldsymbol{x}) \text{ (regular)} \quad \forall \boldsymbol{x} \in \Omega \setminus \Gamma} + \underbrace{\delta_\Gamma(\boldsymbol{x})\, ([\![\boldsymbol{u}]\!](\boldsymbol{x}) \otimes \boldsymbol{n})^s}_{\boldsymbol{\varepsilon}_\delta(\boldsymbol{x}) \text{ (singular)} \quad \forall \boldsymbol{x} \in \Gamma} \tag{3}$$

with δ_Γ as the DIRAC-delta function. In eqn (3) it is utilized that $\boldsymbol{\nabla} H_\Gamma = \boldsymbol{n}\ \delta_\Gamma$ and it is assumed that $\boldsymbol{\nabla}^s [\![\boldsymbol{u}]\!](\boldsymbol{x}) = \boldsymbol{0}$, which is justified by the particular finite element implementation. The regular part in eqn (3) is defined for $\boldsymbol{x} \in \Omega \setminus \Gamma$ and can be decomposed following the *enhanced assumed strain* (EAS) concept as

$$\bar{\boldsymbol{\varepsilon}}(\boldsymbol{x}) = \underbrace{\boldsymbol{\nabla}^s \bar{\boldsymbol{u}}(\boldsymbol{x})}_{\hat{\boldsymbol{\varepsilon}} \text{ (compatible)}} - \underbrace{([\![\boldsymbol{u}]\!](\boldsymbol{x}) \otimes \boldsymbol{\nabla}\varphi(\boldsymbol{x}))^s}_{\tilde{\boldsymbol{\varepsilon}}(\boldsymbol{x}) \text{ (enhanced)}} . \tag{4}$$

2.2 Finite element discretization

Finite element discretization of a solid $\mathcal{B}$ is accomplished by employing *elements with embedded discontinuities* [5]. To this end, subdomain Ω_φ is approximated by the band of those elements exhibiting active embedded discontinuities. For a particular element e of this type the displacement field given in eqn (1) is approximated by

$$\boldsymbol{u}^{(e)}(\boldsymbol{x}) \approx \sum_{i=1}^{n_e} N_i^{(e)}(\boldsymbol{x})\ \boldsymbol{d}_i + [H_\Gamma^{(e)}(\boldsymbol{x}) - \varphi^{(e)}(\boldsymbol{x})]\ [\![\boldsymbol{u}]\!]_\Gamma^{(e)} \tag{5}$$

with $N_i^{(e)}$ as the standard interpolation function associated with node i and the respective displacement vector $\boldsymbol{d}_i$. Displacement field $[\![\boldsymbol{u}]\!]$ in eqn (1) is approximated through vector $[\![\boldsymbol{u}]\!]_\Gamma^{(e)}$ considered to be constant within element e (which justifies assuming $\boldsymbol{\nabla}^s [\![\boldsymbol{u}]\!] = \boldsymbol{0}$ in eqn (3)) and defined as

$$[\![\boldsymbol{u}]\!]_\Gamma^{(e)} = \zeta^{(e)} \cdot \boldsymbol{m}^{(e)} \tag{6}$$

with $\zeta^{(e)}$ as the amplitude of the displacement jump associated with element e and $\boldsymbol{m}^{(e)}$ as the respective direction unit vector. In the simplest case – corresponding to mode-I fracture – considering only normal crack openings across Γ, $\boldsymbol{m} \equiv \boldsymbol{n}$ holds. In order to fulfill eqn (2) function $\varphi^{(e)}$ is approximated by

$$\varphi^{(e)} = \sum_{i=1}^{n_e^+} N_i \tag{7}$$

with the right hand side representing the sum of the standard shape functions N_i associated with those nodes of element e located at the positive side of $\Gamma^{(e)}$. With eqns (1) and (6) at hand, the regular part of the strain field $\bar{\boldsymbol{\varepsilon}}$ in eqn (4) can be written for element e as

$$\bar{\boldsymbol{\varepsilon}}^{(e)}(\boldsymbol{x}) \approx \underbrace{\sum_{i=1}^{n_e} \left(\boldsymbol{\nabla} N_i^{(e)}(\boldsymbol{x}) \otimes \boldsymbol{d}_i \right)^s}_{\hat{\boldsymbol{\varepsilon}} \text{ compatible}} - \underbrace{\zeta^{(e)} \left(\boldsymbol{\nabla} \varphi^{(e)}(\boldsymbol{x}) \otimes \boldsymbol{m}^{(e)} \right)^s}_{\tilde{\boldsymbol{\varepsilon}} \text{ enhanced}} \tag{8}$$

with $\boldsymbol{\nabla}\varphi^{(e)} = \sum_{i=1}^{n_e^+} \partial_{\boldsymbol{x}} N_i$ following from eqn (7).

2.3 Solving for the displacement jump

In eqn (8) the magnitude of the displacement jump $\zeta^{(e)}$ can be determined by employing a standard return mapping procedure [6]. To this end the compatible part $\hat{\boldsymbol{\varepsilon}}$ of the regular strain field in eqn (8) is considered as the elastic strain, whereas the enhanced part $\tilde{\boldsymbol{\varepsilon}}$ is interpreted as the inelastic strain [7]. Hence, the magnitudes of the displacement jumps $\zeta^{(e)}$ can be solved independently for each element indicating cracking [2]. It is emphasized that the present formulation is based on the fixed crack concept with vector $\boldsymbol{m}^{(e)}$ in eqn (8) considered as invariable with respect to time.

3 TRACKING OF DISCONTINUITY SURFACES

In [2] it is shown that discontinuity segments $\Gamma^{(e)}$ cannot be arbitrarily placed within individual element domains. In order to obtain objective, i.e. mesh-independent, results it is rather necessary to enforce continuity of discontinuity segments across adjacent element faces such that a physical discontinuity, i.e. a macroscopic crack, is geometrically represented by the C^0-continuous approximation

$$\Gamma \approx \bigcup_{i=1}^{n_{elem}^{dis}} \Gamma^e \tag{9}$$

with n_{elem}^{dis} as the number of those elements exhibiting a displacement discontinuity, i.e. those forming Ω_φ. A discontinuity is considered to emerge from a certain material point, i.e. its *root*. In a finite element setting the root is established by the *root element*, i.e. that element, for which cracking is indicated and which cannot be joined with one of the existing discontinuities.

3.1 The partial domain tracking algorithm

In order to enforce continuity of discontinuity surfaces so called *tracking algorithms* [3] are used. In [4] a *partial domain tracking algorithm* (PDTA) was proposed and the necessary steps were outlined for tracking of discontinuities across two-dimensional discretizations employing linear triangular elements. Within this algorithm – similar to the *global tracking algorithm* [3] – a particular discontinuity surface is represented by the isosurface of a scalar field $\theta(\boldsymbol{x})$. In contrast to the global tracking algorithm, however, this scalar field is constructed only within those elements that are actually or potentially will be affected by the discontinuity surface. In the following the algorithm will be outlined for three-dimensional discretizations employing linear tetrahedron (four node) elements.

For an element e – crossed by a discontinuity surface – the scalar field $\theta^{(e)}$ must fulfill

$$\begin{aligned} \boldsymbol{s}^{(e)} \cdot \boldsymbol{\nabla}\theta^{(e)} &= 0 \\ \boldsymbol{t}^{(e)} \cdot \boldsymbol{\nabla}\theta^{(e)} &= 0, \end{aligned} \tag{10}$$

where $\boldsymbol{s}^{(e)}$ and $\boldsymbol{t}^{(e)}$ denote a set of vectors in the plane of the discontinuity segment $\Gamma^{(e)}$. Conse-

quently,

$$\boldsymbol{n}^{(e)} \cdot \boldsymbol{s}^{(e)} = \boldsymbol{n}^{(e)} \cdot \boldsymbol{t}^{(e)} = 0 \tag{11}$$

holds and for the scalar field $\theta^{(e)}$ within element e it follows that

$$\boldsymbol{\nabla}\theta^{(e)} = c \cdot \boldsymbol{n}^{(e)} \quad c \in \mathbb{R}^{+}. \tag{12}$$

Construction of scalar field $\theta(\boldsymbol{x})$ is established sequentially starting from the root element for which $\theta^{(e=r)}$ is found according to (12) by prescribing an arbitrary value $\theta_\Gamma \in \mathbb{R}$ at its centroid and an arbitrary value $c \in \mathbb{R}^{+}$. Then, element $e+1$ exhibiting face-connectivity with element $e = r$ is identified. The scalar field $\theta^{(e+1)}$ is already known at the nodes of the common face with element e and is undetermined only at one single node. Thus, for element $e+1$ eqn (12), in general, cannot be fulfilled for any c. Hence, eqn (12) is replaced by the optimization problem

$$\|\boldsymbol{\eta}\|^{(e+1)} = \|\boldsymbol{\nabla}\theta^{(e+1)} - c \cdot \boldsymbol{n}^{(e+1)}\| \rightarrow \min, \tag{13}$$

minimizing the norm of vector $\boldsymbol{\eta}^{(e+1)}$ representing the deviation between the gradient of field $\theta^{(e+1)}$ and the discontinuity normal vector $\boldsymbol{n}^{(e+1)}$. In [2] a possible approach to solve eqn (13) for the single nodal scalar value is given. The above procedure is repeated until for a particular element no adjacent element can be found, i.e. until the boundaries of the discretized domain are reached.

Once field $\theta(\boldsymbol{x})$ is constructed it can be exploited at element level for determining the position of discontinuity segment $\Gamma^{(e)}$ and the set of the nodes located at the positive side of $\Gamma^{(e)}$ in order to derive function $\varphi^{(e)}$ in eqn (7). Since $\Gamma^{(e)}$ is represented by the isosurface $\theta_\Gamma = \text{const}$ for $\varphi^{(e)}$

$$\varphi^{(e)} = \sum_{i=1}^{n_e^+} N_i \quad \text{with} \quad n_e^+ : n_k | \theta_k - \theta_\Gamma > 0 \tag{14}$$

must hold.

3.2 Academic examples

Construction of field $\theta(\boldsymbol{x})$ is shown by tracking given discontinuities within a cube of dimension L occupying $\Omega \subset \mathbb{R}^3$ and regularly discretized by $n_{elem} = 1500$ linear tetrahedron elements as shown in Fig. 1a. One of the elements serves as a root element r associated with discontinuity Γ as

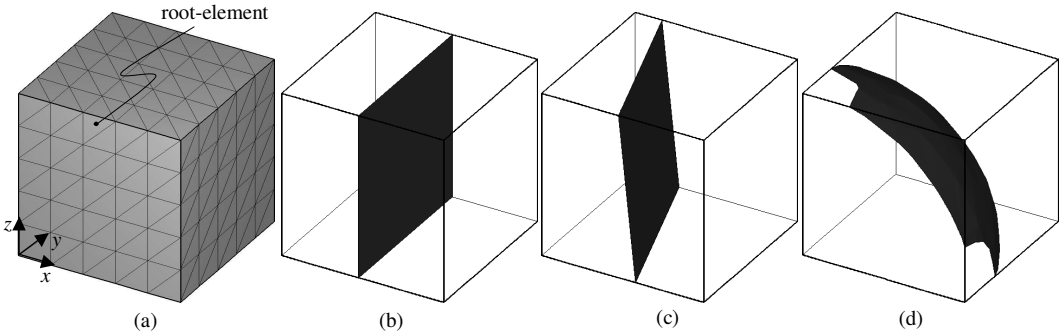

Figure 1: Numerical study of discontinuity tracking for three-dimensional discretizations: (a) cubic domain discretized with linear tetrahedron elements; isosurfaces $\theta_\Gamma = \text{const}$ for discontinuity surfaces prescribed by (b) a vertical plane, (c) an inclined plane, (d) a sphere.

indicated in Fig. 1a. Tracking of the discontinuity is investigated for three cases of imposed discontinuity normal vectors $\boldsymbol{n}^{(e)} \quad \forall e \in \{1 \dots n_{elem}\}$: (i) $\boldsymbol{n}^{(e)} = \lfloor 1,\ 0,\ 0 \rfloor^T$ describing a vertical, plane discontinuity surface, (ii) $\boldsymbol{n}^{(e)} = \lfloor 0.925,\ 0.337,\ 0.174 \rfloor^T$ describing an inclined plane discontinuity surface and (iii) $\boldsymbol{n}^{(e)} = \boldsymbol{x}^{(e)}_{cen} / \| \boldsymbol{x}^{(e)}_{cen} \|$ with $\boldsymbol{x}^{(e)}_{cen}$ as the coordinates of the centroid of element e and hence describing a spherical discontinuity surface. The isosurfaces associated with the scalar value imposed at the centroid of root r corresponding to the three different cases are depicted in Figs. 1b-d. It is seen that in all cases the discontinuity surface described by the imposed normal vectors is nicely reproduced by the respective isosurface. Since in the first two cases a plane surface is obtained, $\| \boldsymbol{\eta} \|^{(e)} = 0 \quad \forall e \in \{1 \dots n^{elem}_{dis}\}$ holds. For the spherical surface $\| \boldsymbol{\eta} \|^{(e)} \neq 0$. However, $\| \boldsymbol{\eta} \|^{(e)}$ is small, not exceeding $2 \cdot 10^{-2}$. It is emphasized that this is not a drawback but an essential consequence of the algorithm.

4 NUMERICAL EXAMPLE

Application of the proposed algorithm to tracking of an arbitrary 3D-crack surface is now shown for the numerical simulation of the *PCT-3D*-experiment [2]. The experiment was conducted on a beam-shaped specimen (600/180/180 mm) with a triangular notch placed eccentrically both in transversal and longitudinal direction. The load is applied as a point load also acting eccentrically in transversal and longitudinal direction. As a result a doubly curved crack-surface is obtained [2]. The tracking algorithm is applied to a finite element discretization of the specimen characterized by 14034 linear

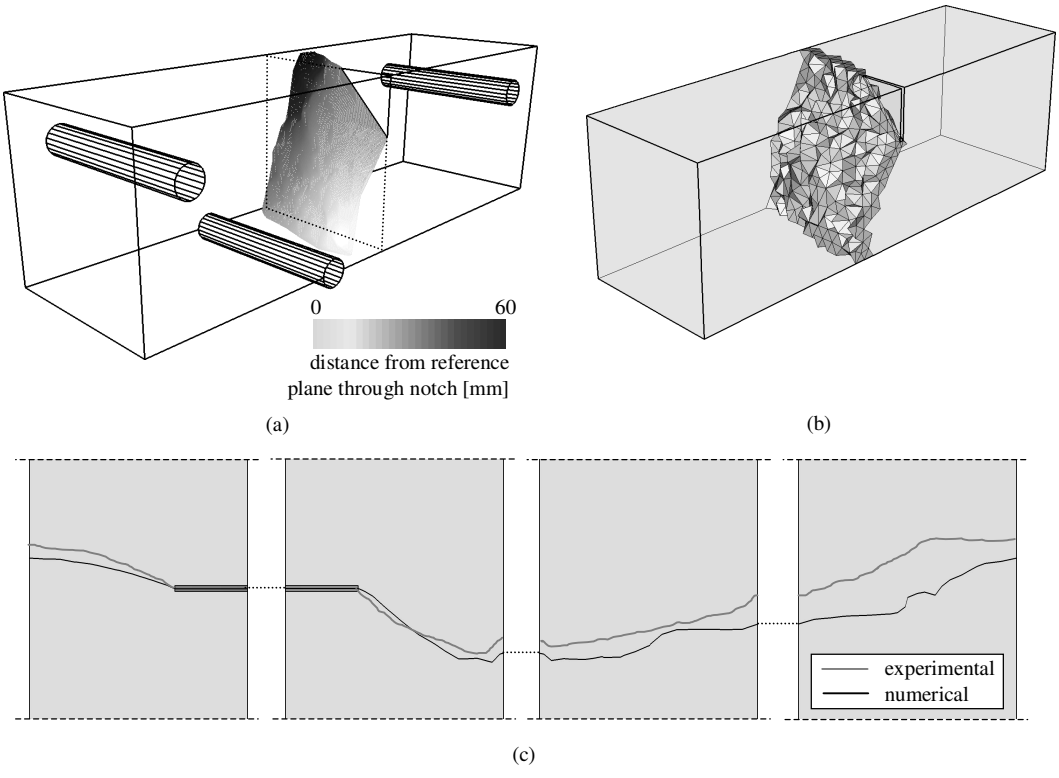

Figure 2: Experiment PCT-3D: (a) crack surface observed at the specimen, (b) elements identified by the PDTA as crossed by the discontinuity surface.

tetrahedron elements and 2794 nodes.

The experimentally obtained crack surface is depicted in Fig. 2a. Application of the PDTA to the finite element discretization allows to identify those elements that are actually or potentially will be crossed by the doubly curved discontinuity surface (Fig. 2b). As can be seen the respective partial domain shows a very good agreement with the experimentally obtained crack-surface. The good correspondence is even more evident from the comparison of the experimentally obtained and numerically resolved trace of the crack-surface along the developed surface (rotated counterclockwise by 90 $^\circ$) of the specimen given in Fig. 2c.

5 CONCLUSIONS AND OUTLOOK

A numerical model formulated within the Strong Discontinuity Approach for three-dimensional fracture simulations was outlined. In order to enforce a C^0-continuous geometric representation of a particular discontinuity surface, a tracking algorithm was devised. Within this algorithm the discontinuity surface is represented by the isosurface of a scalar field which is constructed over a certain subdomain of the domain under consideration for the mechanical problem. Hence, it was termed as a *partial domain tracking algorithm* (PDTA). Its basic capabilities were shown by some academic examples. Application of the algorithm to a problem involving an arbitrarily shaped, 3D crack-surface demonstrated its general capabilities.

REFERENCES

[1] E. Samaniego. *Contributions to the Continuum Modelling of Strong Discontinuities in Two-dimensional Solids*. PhD thesis, UPC Barcelona, 2003.

[2] C. Feist. *A Numerical Model for Cracking of Plain Concrete Based on the Strong Discontinuity Approach*. PhD thesis, Universität Innsbruck, 2004.

[3] J. Oliver, A. E. Huespe, E. Samaniego, and E. W. V. Chaves. On strategies for tracking strong discontinuities in computational failure mechanics. In H.A. Mang, F.G. Rammerstorfer, and J. Eberhardsteiner, editors, *Proc.World Congress on Computational Mechanics, WCCM V*, Austria, 2002. Vienna University of Technology. http://wccm.tuwien.ac.at.

[4] C. Feist and G. Hofstetter. Mesh-insensitive strong discontinuity approach for fracture simulations of concrete. In *Numerical Methods in Continuum Mechanics, NMCM 2003*, 2003. CD-Rom.

[5] M. Jirásek. Comparative study on finite elements with embedded discontinuities. *Computer Methods in Applied Mechanics and Engineering*, 188(1-3):307–330, 2000.

[6] J.C. Simo and T.J.R. Hughes. *Computational Inelasticity*, volume 7. Springer, New York, 1998.

[7] J. Mosler. *Finite Elemente mit sprungstetigen Abbildungen des Verschiebungsfeldes für numerische Analysen lokalisierter Versagenszustände in Tragwerken*. PhD thesis, Ruhr-Universität Bochum, 2002. in German.